Novel technique to average breathing loops for infant respiratory function testing

G. Schmalisch **M. Schmidt** **B. Foitzik**

Clinic of Neonatology (Charité), Humboldt University, Berlin, Germany

Abstract—*Breathing loops can be obtained by plotting two respiratory signals on an x–y diagram: the resulting loops represent a non-parametric description of the respiratory system. In infancy, loops are commonly measured during tidal breathing and their interpretation is hampered by high within-subject variability. Therefore a two-dimensional averaging technique for loops has been developed. The algorithm is based on segmentation of the loops and required two steps. First, the total length of the loop of every breathing cycle was divided into a specified number of equidistant intervals and the co-ordinates calculated by stepwise linear approximation of the curve. Second, averaged loops were calculated using the arithmetical mean (or the median if there were artifacts) of the x and y co-ordinates of the loops for all calculated points. To compare the new technique with averaging in the time domain a simulation study was performed using respiratory signals with a coefficient of variation (CV) of 5%, 10%, 15% and 20%. In contrast to the new technique, with increasing CV, averaging in the time domain led to increasing contortions in the averaged flow-volume loops. Mean errors of peak tidal expiratory flow were −3.3%, −13.9%, −21.3% and −34.2%, whereas errors with the new technique were considerably lower (0.5%, 0.4%, 0.5% and −0.1%) and independent of the level of CV.*

Keywords—*Lung function testing, Breathing loops, Ventilation, Lung mechanics, Averaging techniques, Data processing, Newborns*

Med. Biol. Eng. Comput., 2001, **39**, 688–693

1 Introduction

RESPIRATORY DISEASES in newborns are an important factor in neonatal morbidity and mortality (GNANARATNEM and FINER, 2000) as well as in infants after intensive care (GREENOUGH, 2000). Since commercial pulmonary function devices became available several years ago, there has been increasing clinical interest in infant respiratory function testing (RFT) for clinical and research purposes.

The four fundamental respiratory signals which describe ventilation and lung mechanics are volume $V(t)$, air flow $\dot{V}(t)$, gas acceleration $\ddot{V}(t)$ and the pulmonary driving pressure $P(t)$ required to achieve the ventilation. These four signals which can be described approximately by the general equation of motion

$$I \cdot \ddot{V}(t) + R \cdot \dot{V}(t)) + \frac{1}{C} V(t) = P(t) \tag{1}$$

where I = inertance of the air and the tissue, R = air flow and tissue frictional resistance, C = compliance of the lung (spontaneous breathing), or lung and chest wall (mechanical ventilation). The adequacy of this single-compartment model is an essential prerequisite of many RFTs. However, in sick infants this assumption is often not fulfilled (e.g. due to non-linearities or pulmonary inhomogeneities) which can lead to significant measurement errors in lung mechanics parameters, wrong diagnosis and possible misdirection of therapies. Then, a non-parametric description of the measurements is more informative (e.g. static pressure–volume curves, breathing loops, frequency response of respiratory impedance).

Breathing loops are the simplest non-parametric representation of the respiratory system and they result from the x–y representation of two respiratory signals. Infants are commonly investigated during tidal breathing so that the inertial forces are negligible compared with the elastic and resistive forces of lung mechanics (LANTERI *et al.*, 1999). Therefore for RFT only flow–volume, pressure–flow and pressure–volume loops were considered. Nevertheless, x–y diagrams of higher order derivatives of $V(t)$ (e.g. $\ddot{V}(t)-\dddot{V}(t)$ diagrams) can advantageously be used to investigate the control of breathing by methods from non-linear dynamics (SAMMON *et al.*, 1993). Further breathing loops can be obtained by measurement of chest wall and abdominal movements (HERSHENSON *et al.*, 1990). Every breathing cycle produces a more or less closed loop in an x–y diagram and the shape of the loops provides insight into the dynamic behaviour of the respiratory system.

For a parametric evaluation of RFTs (e.g. determination of ventilatory or lung mechanical parameters) the mean or median of a number of breathing cycles is commonly calculated.

Correspondence should be addressed to Dr sc nat G. Schmalisch; email: gerd.schmalisch@charite.de

Paper received 30 August 2001

MBEC online number: 20013624

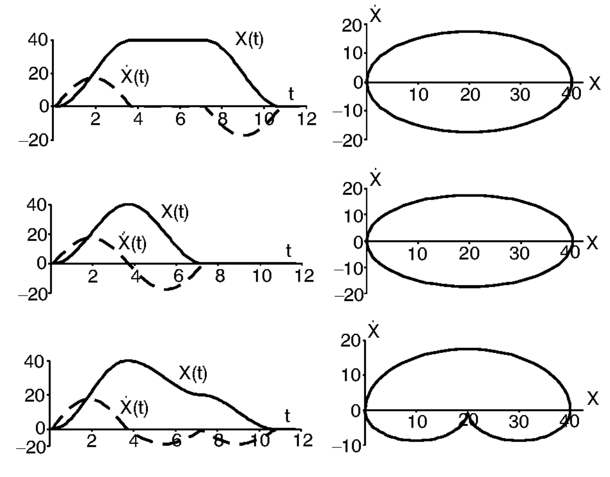

Fig. 1 *Two different sinusoidal velocity signals $\dot{x}(t)$ (– – – –) and their integral x(t) (———) with identical elliptical X–Ẋ loops (top and middle) were averaged in the time domain (bottom). The loop of the averaged time signal differs significantly from an elliptical shape*

However, for non-parametric evaluations this procedure cannot be adopted as easily because there are no standardised algorithms to average loops.

Averaging the measured signals in the time domain is the simplest way to obtain a 'representative' breathing cycle. However, unexpected contortions can occur in the loops as shown in Fig. 1. Important sources of contortions are breath-to-breath variability in the respiratory rate or inspiratory–expiratory time ratio. The aim of this study was therefore to develop and to validate a time-independent algorithm to average breathing loops in the x–y plane.

2 Averaging breathing loops

The shape of breathing loops can be very complex (e.g. crossing points, deformation by artifacts). Therefore, no assumptions about the shape of the loop were made. The algorithm developed is independent of the loop's shape and the following two steps are required:

1. Segmentation of each loop into a fixed number, K, of equidistant intervals and calculation of new co-ordinates for each interval.
2. Determination of the averaged loop by calculating the mean or median of the x and y co-ordinates of all calculated points with the same index.

The segmentation of loops requires first the calculation of their length. Generally, the length L_C of a curve in the time interval T described by the signals $x(t)$ and $y(t)$ is given by

$$L_C = \int_{t_0}^{t_0+T} \sqrt{\dot{x}^2(t) + \dot{y}^2(t)}dt \tag{2}$$

For computerized measurements of breathing loops the signals $x(t)$ and $y(t)$ were sampled with an equidistant time interval Δt and the duration of the breathing cycle is given by $T = N \cdot \Delta t$, where N is the number of samples per cycle. Eqn 2 can be written as

$$L = \sum_{i=0}^{N-1} \sqrt{(((x(i+1) - x(i))^2 + ((y(i+1) - y(i))^2)} \tag{3}$$

using the sample values $x(i), y(i)$ with $i = 0, 1, \ldots, N$.

Afterwards the whole loop is divided into K segments of the same length $l_{\text{equi}} = L/K$. The number of segments K may be lower than, higher than or equal to the number of sampling intervals. Calculation of the starting point $x(j), y(j)$ and the end point $x(j+1), y(j+1), j = 0, 1, \ldots, K-1$, of each segment is based on the original sample points $x(i), y(i)$ $(i = 0, 1, 2, \ldots, N)$. As shown in Fig. 2, for each end point $x(j+1), y(j+1)$ of a segment with the length l_{equi}, both neighbouring points of the values originally sampled $x^*(i)$, $y^*(i)$ and $x^*(i+1)$, $y^*(i+1)$ have to be found by a suitable search strategy. Then the co-ordinates can be calculated using

$$x(j+1) = x^*(i) + l_a \times \frac{x^*(i+1) - x^*(i)}{\sqrt{(x^*(i+1) - x^*(i))^2 + (y^*(i+1) - y^*(i))^2}}$$

$$y(j+1) = y^*(i) + l_a \times \frac{y^*(i+1) - y^*(i)}{\sqrt{(x^*(i+1) - x^*(i))^2 + (y^*(i+1) - y^*(i))^2}} \tag{4}$$

The unknown length l_a between $x^*(i)$, $y^*(i)$ and the new end point $x(j+1), y(j+1)$ can be determined using the cosine rule (Fig. 2)

$$l_{\text{equi}}^2 = l_a^2 + l_b^2 + 2 \cdot l_a l_b \cos(\gamma) \tag{5}$$

where l_b is the length between the starting point $x(j)$, $y(j)$ and $x^*(i), y^*(i)$

$$l_b = \sqrt{(x(j) - x^*(i))^2 + (y(j) - y^*(i))^2} \tag{6}$$

and

$$\cos(\gamma) = \frac{(x^*(i+1) - x^*(i))(x(j) - x^*(i)) + (y^*(i+1) - y^*(i))(y(j) - y^*(i))}{\sqrt{[(x^*(i+1) - x^*(i))^2 + (y^*(i+1) - y^*(i))^2] \times [(x(j) - x^*(i))^2 + (y(j) - y^*(i))^2]}} \tag{7}$$

If $l_b = 0$ (i.e. $x^*(i) = x(j)$ and $y^*(i) = y(j)$) then the length l_a is identical to l_{equi}. If $l_b > 0$ then the length l_a is a solution of the quadratic equation (eqn 5):

$$l_a = l_b \cdot \cos(\gamma) + \sqrt{l_b^2 \cdot (\cos^2(\gamma) - 1) + l_{\text{equi}}^2} \tag{8}$$

Using this algorithm, every curve can be divided into K segments independent of their shape and thus the coordinates $x(j), y(j)$ $(j = 0, 1, 2, \ldots, K)$ can be calculated.

In eqn 3 the curve within the sample intervals is approximated by a straight line. Therefore, the true length of the curve L_C is

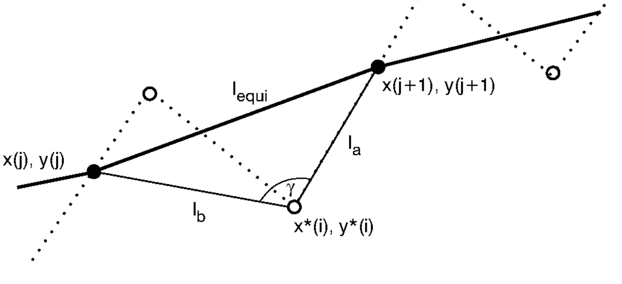

Fig. 2 *Determination of the co-ordinates of equidistant sample points using the cosine rule (original sampled data · · · ·, new sampled data ———)*

always slightly underestimated ($L \leq L_C$). This can lead to a smaller number of calculated segments K^* than the given number of segments K. If the number of sample points is sufficiently high, the reduction will be very small. For clinical purposes it was sufficient to eliminate this error by a new arrangement of the co-ordinates using the linear interpolation

$$\begin{aligned} x_{\mathrm{interpol}}(j) &= x\left[\frac{K^*}{K}j\right] \\ &\quad + \left(x\left[\frac{K^*}{K}j+1\right] - x\left[\frac{K^*}{K}j\right]\right)\left(\frac{K^*}{K}j - \left[\frac{K^*}{K}j\right]\right) \\ y_{\mathrm{interpol}}(j) &= y\left[\frac{K^*}{K}j\right] \\ &\quad + \left(y\left[\frac{K^*}{K}j+1\right] - y\left[\frac{K^*}{K}j\right]\right)\left(\frac{K^*}{K}j - \left[\frac{K^*}{K}j\right]\right) \\ &\qquad \text{with } j = 0, 1, \ldots, K-1 \end{aligned} \quad (9)$$

where [*] indicates the integer value of the brackets. This linear interpolation will change neither the starting point of the curve $x_{\mathrm{interpol}}(0) = x(0)$, $y_{\mathrm{interpol}}(0) = y(0)$ nor the end point $x_{\mathrm{interpol}}(K) = x(K^*)$; $y_{\mathrm{interpol}}(K) = y(K^*)$.

However, we cannot consider the interpolation procedure as an exact solution of the problem since the distances between the sample points (l_{equi}) will be slightly different. Therefore, this correction of the number of sample points K^* can only be used if there is a minimal shortening of the total length L.

The same number of segments K for all loops is an essential prerequisite for calculating the averaged loop of M breathing cycles by the arithmetical mean:

$$\bar{x}(j) = \frac{1}{M}\sum_{m=0}^{m=M} x^m(j) \quad \text{and} \quad \bar{y}(j) = \frac{1}{M}\sum_{m=0}^{m=M} y^m(j) \qquad \text{for } j = 0, 1, \ldots, K \quad (10)$$

or median if there are artifacts in the signals:

$$\begin{aligned} \tilde{x}(j) &= \mathrm{median}[x^1(j),\ x^2(j), \ldots, x^M(j)] \quad \text{and} \\ \tilde{y}(j) &= \mathrm{median}[y^1(j),\ y^2(j), \ldots, y^M(j)] \\ &\qquad \text{for } j = 0, 1, \ldots, K \end{aligned} \quad (11)$$

3 Results

The algorithm developed has been successfully implemented in equipment for lung function testing in newborns (Schmalisch *et al.*, 2001) and can be used to average different types of breathing loops. Fig. 3 shows flow–volume loops of a 100 ml calibration syringe (Hans Rudolph Inc., USA) produced by manual strokes with a constant volume (100 ml) but at different rates. The magnitude of the x axis was almost constant while the magnitude of the y axis changed with the rate. The averaged loop clearly reflects the characteristic of the syringe used. The syringe was in clinical use for a long time and some roughness can be detected in its surface between 40 and 60 ml. This means that the flow–volume loops reflect both the movement of the syringe as well as its mechanical properties. This is the basic idea of the flow–volume loop in RFT.

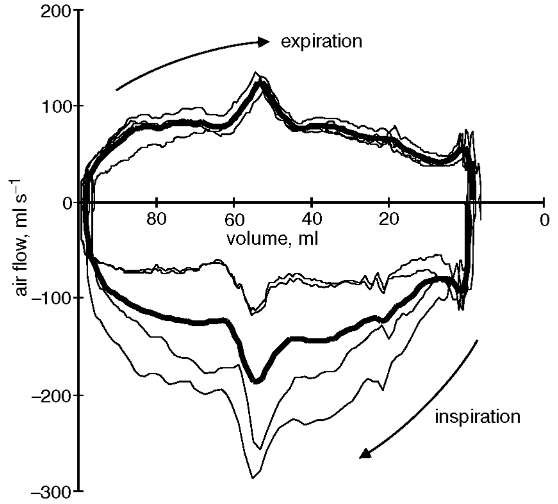

Fig. 3 *Averaged flow–volume loop (thick line) of a calibration syringe with a characteristic chatter mark, using the arithmetical mean. According to clinical standards, the flow–volume begins on the right with inspiration downwards and expiration upwards*

To compare the properties of the algorithm developed with averaging in the time domain a simulation study was performed using flow–volume loops. For this purpose a series of N breathing cycles was generated. Breathing volume $V(t)$ and flow $\dot{V}(t)$ of each cycle were approximated by

$$V(t) = \frac{V_T^i}{2}\left(1 - \cos\frac{2\pi t}{T_i}\right) \quad \text{and} \quad \dot{V}(t) = \frac{V_T^i \cdot \pi}{T_i}\sin\left(\frac{2\pi t}{T_i}\right) \qquad i = 1, 2, \ldots, N \quad (12)$$

where V_T^i are tidal volume and T_i duration of the ith breathing cycle. The corresponding flow–volume loop of each breathing cycle is an ellipse which differ only in width and height. The breath-to-breath variability in depth and respiratory rate was simulated using the equations

$$V_T^i = V_T(1 + \alpha a_i) \quad \text{and} \quad T^i = T(1 + \alpha b_i) \quad (13)$$

where a_i, b_i are independent random numbers in the interval $[-1; 1]$ with

$$\sum_{i=1}^{N} a_i = \sum_{i=1}^{N} b_i = 0$$

and the parameter α ($0 \leq \alpha < 1$) allows adjustment of the variability measured by the coefficient of variation (CV) of the tidal breathing parameters.

For comparative investigations for each given α, ten flow and volume signals with 52 cycles were calculated with the mean $V_T = 15$ ml and the mean $RR = 40\,\mathrm{min}^{-1}$ ($T = 1.5$ s). The parameter α was chosen so that the CV of V_T and RR varies between 1% and 20%. This is the typical range for tidal breathing measurements in sleeping infants (Paetow *et al.*, 1999).

The averaged flow–volume loop of each respiratory signal was calculated using both methods. For averaging in the x–y plane as described in this paper, 300 sample points ($K = 300$) for each loop were used. As shown in Fig. 4, for averaging in the time domain flow and volume signals were aligned at the beginning of inspiration and the signals were averaged separately using a sampling time of 5 ms.

The influence of breath-to-breath variability on the shape of the averaged flow–volume loop is shown in Fig. 5. If the CV was very low (<1%) there was no visible difference between averaging techniques. In contrast to the new averaging technique, with increasing breath-to-breath variability, averaging in the time domain led to distinct contortions, mainly in the expiratory limb. For CV = 20% (sometimes seen in preterm

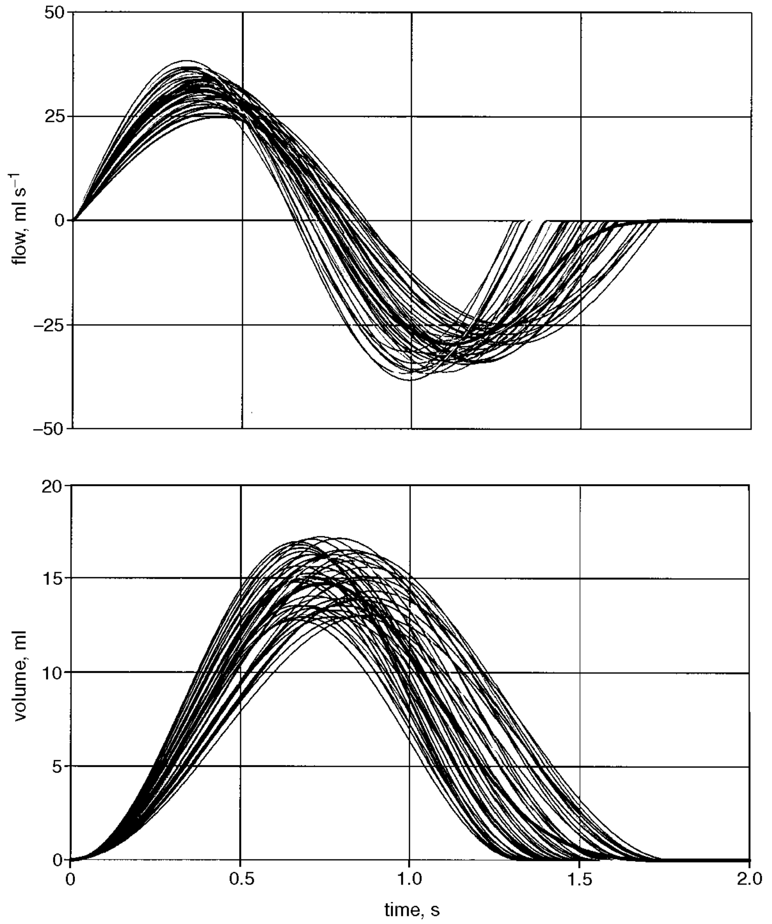

Fig. 4 *Averaging breathing flow (top) and volume (bottom) in the time domain by aligning all breathing cycles ($N = 52$) at the beginning of inspiration. The thick line represents the averaged time profile (coefficient of variation = 10%)*

infants) the contortions of the averaged flow–volume loop are so large that misleading diagnoses are possible.

The influence of breath-to-breath variability on the characteristic parameters of the averaged flow–volume loop are shown in Table 1. Important tidal breathing parameters are the site of the peak inspiratory flow (PTIF) and peak expiratory flow (PTEF) measured by V_{PTIF} and V_{TPEF} (Fig. 5). For an ellipsoid shape the ratios V_{PTEF}/V_T and V_{PTIF}/V_T are exactly 0.5. The errors in the tidal breathing parameters of the averaged loop were considerably different for the two averaging techniques and the highest errors were found in V_{PTEF}. Table 1 shows clearly that the errors in the new averaging technique were independent of the CV of the volume signal, and parameter errors were exclusively caused by numerical errors due to loop sampling, whereas parameter errors when averaging in the time domain increase considerably with increasing CV.

4 Discussion

The algorithm proposed allows one to average breathing loops regardless of their shape, and even in respiratory signals with a high within-subject variability a characteristic loop can be obtained, provided that a sufficient number of breathing cycles was recorded and all loops have nearly the same basic pattern.

The necessary number of breathing cycles depends on the breath-to-breath variability, and the younger the infant, the more irregular is the breathing pattern and the higher the necessary number of breathing cycles. For a parametric evaluation of tidal breathing measurements in infants, STOCKS *et al.* (1994) recommended at least 10 breaths at two separate measuring intervals to obtain representative results.

In contrast to parametric evaluation, not much is known about the influence of within-subject variability on the determination of a representative breathing loop and the necessary number of cycles. Up until now there has not been any approved strategy to determine a representative loop. Instead, in clinical practice, only a few breathing loops have been selected by the investigator for clinical assessment, by considering specified selection criteria (LODRUP-CARLSEN, 1997). However, such user selection has a high risk of subjective bias (AHLSTROM and JONSON, 1974) which can lead to over-evaluation or under-evaluation of any deformations. The advantage of the proposed algorithm is the prevention of any selection bias by the determination of a 'characteristic breathing loop' from a number of consecutive breathing cycles.

As shown in this simulation study, averaging of the time signals to obtain an averaged loop can lead to serious contortions. For a CV of 20% the expiratory limb of the flow–volume loop shown Fig. 5 can wrongly suggest severe airway obstructions and/or pulmonary inhomogeneities characterised by low V_{PTEF}/V_T and a concave expiratory limb. An important source of these contortions is breath-to-breath variability in the respiratory rate. Therefore, BENCHETRIT *et al.* (1989) described, for respiratory flow profiles, averaging in the frequency domain using the fundamental and first three harmonics of each breathing cycle and normalisation of the duration of each breath so that it is of unit length. By this means they showed that the individual breathing pattern in adults is maintained over a long period. SATO and ROBBINS (2001) have previously investigated the characteristics of this technique in detail. A problem of this method is that the reconstructed averaged flow must not be zero at the beginning of inspiration and at the end of expiration so that additional baseline corrections are necessary. Furthermore, the

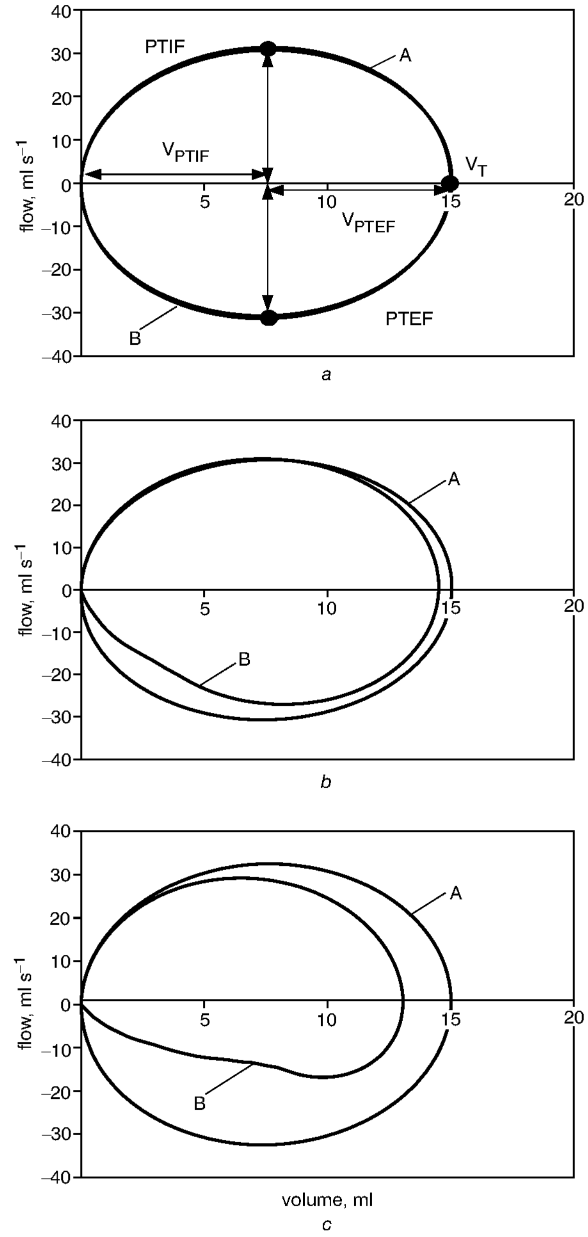

Fig. 5 *Influence of the coefficient of variation (CV) on the shape of the averaged flow–volume loop using the new method (A) and averaging in the time domain (B). The loops are presented in mathematical direction with the start of inspiration at zero on the left side. (Abbreviations of tidal breathing parameters as Table 1.) (a) CV = 1%; (b) CV = 10%; (c) CV = 20%*

requirement for the volume to be the time integral of the flow is lost when flow and volume are averaged separately. To reintroduce this physical law, a numerical correction factor must be calculated.

An improved technique to average flow profiles is described by SATO and ROBBINS (2001). Using normalised flow–volume loops the phase angle of each loop was divided in equidistant intervals. Similarly to the proposed technique, values for flow, volume and the elapsed time since the start of inspiration with the same phase angle were averaged. Using this technique several problems of the Benchetrit method can be avoided, but the technique is limited to loops in which the phase angle during the breathing cycle increases strongly monotonously (e.g. flow–volume loops). The averaging technique described in this paper is independent of the shape of the loop and can also be used in loops with crossing points (e.g. pressure–flow loops).

In contrast to the intention of this paper, in the averaging techniques suggested by Benchetrit and by Sato and Robbins the determination of characteristic time profiles of respiratory flow and volume is the centre of interest and not the determination of an averaged breathing loop. Our approach based on average breathing loops assumes the existence of a typical pattern in all consecutively measured breathing cycles independent of their size. Along with most other researches in this field it is assumed that breathing loops registered during tidal breathing do not cluster into several loop patterns. However, this assumption is difficult to verify.

Even during tidal breathing the assumption of stationarity of the respiratory signals need not necessarily always be fulfilled (KHOO, 2000). The highest changeability seems to be in the control of breathing. Some studies have shown that respiratory control is more a deterministic than a stochastic process, which can lead to changes in the breathing pattern (SAMMON, 1994; SMALL *et al.*, 1999). Because the probability of deterministic changes in the breathing pattern exists, a visual inspection of all recorded loops by the investigator is necessary. Single breathing loops which differ significantly from all other loops (e.g. sighs) can be excluded by robust methods of averaging (use of the median instead of the mean).

The algorithm developed has been used successfully in equipment for lung function testing in newborns for over five years (SCHMALISCH *et al.*, 2001). The sample rate of the measured signals was 200 Hz and for averaging the breathing loops $K = 400$ data points were used, independent of the respiratory rate. The resulting resolution of the loops was sufficient for detailed qualitative investigations. Using this averaging technique we were able to investigate the variability of tidal breathing flow–volume loops in healthy and sick newborns (PAETOW *et al.*, 1999) or the lung mechanics during

Table 1 Parameter errors of the averaged flow–volume curves by averaging in the time domain and by the new averaging in the x–y plane (data in brackets). Presented are group means ± standard deviation of 10 simulated breathing patterns with coefficients of variation (CV) of 5%, 10%, 15% and 20%

	Errors, %			
Parameter	CV = 5%	CV = 10%	CV = 15%	CV = 20%
δV_T	−0.7 ± 0.05	−3.3 ± 0.3	−5.4 ± 0.4	−10.3 ± 0.9
	(0.3 ± 0.9)	(−0.4 ± 1.0)	(−0.1 ± 1.2)	(0.5 ± 2.5)
δPTIF	−0.4 ± 0.03	−1.6 ± 0.1	−2.6 ± 0.2	−5.0 ± 1.3
	(0.5 ± 1.1)	(0.4 ± 1.1)	(0.5 ± 1.9)	(−0.1 ± 4.1)
δPTEF	−3.3 ± 0.2	−13.9 ± 1.1	−21.3 ± 1.8	−34.2 ± 4.7
	(0.5 ± 1.1)	(0.4 ± 1.1)	(0.5 ± 1.9)	(−0.1 ± 4.1%)
δV_{PTIF}	−3.5 ± 0.2	−4.4 ± 0.7	−6.2 ± 1.3	−9.9 ± 1.1
	(−0.2 ± 0.9)	(0.1 ± 1.3)	(−0.2 ± 1.1)	(1.1 ± 2.4)
δV_{PTEF}	−3.7 ± 0.2	−16.0 ± 2.2	−25.8 ± 1.3	−46.6 ± 5.2
	(−4.0 ± 0.8)	(−4.7 ± 0.9)	(−4.3 ± 1.2)	(−2.8 ± 2.4)

Abbreviations: V_T – tidal volume, *PTIF* – peak tidal inspiratory flow, *PTEF* – peak tidal expiratory flow, V_{PTIF} – inspired volume to PTIF, V_{PTEF} – expired volume to PTEF

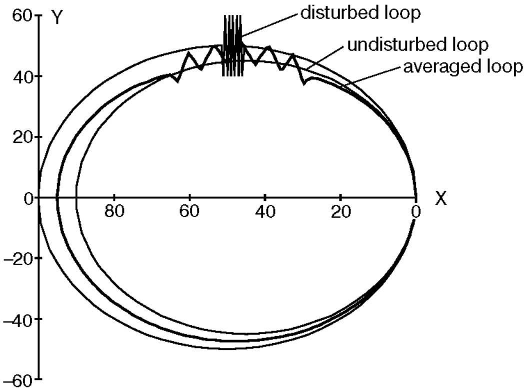

Fig. 6 *Influence of local disturbances on the averaged loop calculated from an undisturbed and a disturbed loop*

mechanical ventilation using pressure–volume or pressure–flow loops (Foitzik *et al.*, 1998). Clinical experience has shown that the algorithm works reliably if the above mentioned prerequisites are fulfilled. Only local disturbances which increase the total length of the loop significantly can lead to unexpected contortions. As shown in Fig. 6, a local disturbance can be spread over enlarged parts of the averaged loop.

One important advantage of this algorithm is that it can also be used for segments of a curve and does not require a closed loop. Separate determination of the inspiratory and expiratory limb can be useful to prevent any mutual influence between both parts of the respiratory cycle. The algorithm described has already been applied successfully to very complex loop patterns and its application is not limited to lung function testing.

Acknowledgment—This work was supported by the German Ministry of Education and Research (BMBF), research project 'Perinatal Lung' (01 ZZ 9511).

References

Ahlstrom, H., and Jonson, B. (1974): 'Pulmonary mechanics in infants. Methodological aspects', *Scand. J. Respir. Dis.*, **55**, pp. 129–140

Benchetrit, G., Shea, S. A., Dinh, T. P., Bodocco, S., Baconnier, P., and Guz, A. (1989): 'Individuality of breathing patterns in adults assessed over time', *Respir. Physiol.*, **75**, pp. 199–209

Foitzik, B., Schmidt, M., Proquitte, H., and Schmalisch, G. (1998): 'Interactive computer program for separating respiratory pressure in newborn infants into its elastic, viscous and inert components', *Biomed. Tech.*, **43**, pp. 278–279

Gnanaratnem, J., and Finer, N. N. (2000): 'Neonatal acute respiratory failure', *Curr. Opin. Pediatr.*, **12**, pp. 227–232

Greenough, A. (2000): 'Measuring respiratory outcome', *Semin. Neonatol.*, **5**, pp. 119–126

Hershenson, M. B., Colin, A. A., Wohl, M. E., and Stark, A. R. (1990): 'Changes in the contribution of the rib cage to tidal breathing during infancy', *Am. Rev. Respir. Dis.*, **141**, pp. 922–925

Khoo, M. C. (2000): 'Determinants of ventilatory instability and variability', *Respir. Physiol.*, **122**, pp. 167–182

Lanteri, C. J., Petak, F., Gurrin, L., and Sly, P. D. (1999): 'Influence of inertance on respiratory mechanics measurements in mechanically ventilated puppies', *Pediatr. Pulmonol.*, **28**, pp. 130–138

Lodrup-Carlsen, K. C. (1997): 'Tidal breathing analysis in infants and preschool children: tidal flow-volume loops' in Zach, M., Carlsen, K. H., Warner, J. O., and Sennhauser, F. H. (Eds): 'New diagnostic techniques in paediatric respiratory medicine' (ERS Monograph 5, ERS Journals, Sheffield), pp. 27–57

Paetow, U., Windstetter, D., and Schmalisch, G. (1999): 'Variability of tidal breathing flow-volume loops in healthy and sick newborns', *Am. J. Perinatol.*, **16**, pp. 549–559

Sammon, M. (1994): 'Symmetry, bifurcations, and chaos in a distributed respiratory control system', *J. Appl. Physiol.*, **77**, pp. 2481–2495

Sammon, M., Romaniuk, J. R., and Bruce, E. N. (1993): 'Bifurcations of the respiratory pattern associated with reduced lung volume in the rat', *J. Appl. Physiol.*, **75**, pp. 887–901

Sato, J., and Robbins, P. A. (2001): 'Methods for averaging irregular respiratory flow profiles in awake humans', *J. Appl. Physiol.*, **90**, pp. 705–712

Schmalisch, G., Foitzik, B., Wauer, R. R., and Stocks, J. (2001): 'Effect of apparatus dead space on breathing parameters in newborns: "flow-through" versus conventional techniques', *Eur. Respir. J.*, **17**, pp. 108–114

Small, M., Judd, K., Lowe, M., and Stick, S. (1999): 'Is breathing in infants chaotic? Dimension estimates for respiratory patterns during quiet sleep', *J. Appl. Physiol.*, **86**, pp. 359–376

Stocks, J., Dezateux, C. A., Jackson, E. A., Hoo, A. F., Costeloe, K. L., and Wade, A. M. (1994): 'Analysis of tidal breathing parameters in infancy: how variable is t_{PTEF}/t_E', *Am. J. Respir. Crit. Care Med.*, **150**, pp. 1347–1354

Authors' biographies

Gerd Schmalisch is a university lecturer at the Clinic of Neonatology (Charité) of the Humboldt University Berlin. He received his Dr.-Ing. in Cybernetics from the Technical University Dresden in 1979 and his Dr.sc.nat. in Biophysics from the Humboldt-University Berlin in 1990. His scientific fields are biomathematics, biological modelling, surface tension measurements and respiratory physiology. Since 1992 he has been the head of an interdisciplinary research laboratory for infant respiratory function testing, and headed several research projects in this field.

Mario Schmidt received his Diploma in Informatics from the Humboldt-University Berlin in 1995. His main research interests include signal processing, pattern recognition, and forced oscillation techniques. He received his Dr.-Ing. in Technical Informatics from the Humboldt-University Berlin in 2000.

Bertram Foitzik qualified as a bioengineer from the Technical University Dresden in 1992 and received his Dr.-Ing. in Technical Informatics from the Humboldt-University Berlin in 2001. His research interests are in the development of equipment for respiratory function testing in infants, and respiratory signal processing.